



MOX–Report No. 65/2013

## Plasticity in passive cell mechanics

AMBROSI, D.; CIARLETTA, P.

MOX, Dipartimento di Matematica “F. Brioschi”  
Politecnico di Milano, Via Bonardi 9 - 20133 Milano (Italy)

[mox@mate.polimi.it](mailto:mox@mate.polimi.it)

<http://mox.polimi.it>



# Plasticity in Passive Cell Mechanics

D. Ambrosi<sup>a</sup>, P. Ciarletta<sup>b,c</sup>

<sup>a</sup> *MOX-Dipartimento di Matematica, Politecnico di Milano,  
piazza Leonardo da Vinci 32, 20133 Milano, Italy*

<sup>b</sup> *CNRS and Institut Jean le Rond d'Alembert, UMR 7190, Université Pierre et Marie Curie - Paris 6  
4 place Jusseu, Case 162, 75005 Paris, France*

<sup>c</sup> *CEN - Centro Europeo di Nanomedicina, via Taramelli 12 F, 20124 Milano, Italy*

---

## Abstract

A sufficiently large load applied to a living cell for a sufficiently long time produces a deformation which is not entirely recoverable by passive mechanisms. This kind of plastic behavior is well documented by experiments but is still seldom investigated in terms of mechanical theories. Here we discuss a finite visco-elasto-plastic model where the rest elongation of the cell evolves in time as a function of the dissipated energy at a microstructural level. The theoretical predictions of the proposed model reproduce, also in quantitative terms, the passive mechanics of optically stretched cells.

*Keywords:* living cell, visco-elasto-plasticity, cell mechanics, plastic hardening  
*2000 MSC:* 74C20, 92C05

---

## 1. Introduction

The mechanical characterization of eukaryotic cells has been the subject of a number of studies in the last twenty years [1]. The variety of experimental techniques utilized and the resulting extensive literature is not surprising when considering the relevance and the complexity of this biophysical system. Standard stress-strain plots can be produced by a number of different techniques, exploring a wide range of stress and strain, in magnitude and frequency. However an attempt to explain the results in terms of classical linear spring-dashpots models might be frustrated by the richness of the observed behaviors, due to the many inner mechanisms that concur in producing the apparent mechanical behavior. The most relevant features of cell mechanics are listed below.

- The mechanical behavior of a cell is the superposition of the mechanical response of various components: actin filaments, microtubules, intermediate filaments, each one having a different location in the cell. The observed overall dynamics is actually produced by a strongly non-homogeneous structure.
- Crosslinking proteins couple the mechanics of the phases, producing a global response that is not the mere superposition of the contributions of the single components. Even

if the mechanical properties of the cell partially correspond to those of networks of purified cytoskeletal components, large discrepancies exist

- Different cell lines and experimental techniques produce behaviors that can be difficult to set in a unified framework. [2].
- Motor proteins inside a cell, and actomyosin complexes in particular, give raise to an active dynamic contribution that is the signature of living matter. This peculiarity poses intriguing questions about the actual meaning of the stress measures.

A substantial advance in the understanding of cell mechanics has been obtained by dynamic rheology: applying forces at given frequencies, it has been possible to characterize the shear storage modulus  $G'$  over several frequency ranges with a wide consensus. The main result is that  $G'$  depends on the frequency  $f$  according to a power law  $G' \propto f^\beta$ , the exponent  $\beta$  being universally recast between 0.2 and 0.3. The same results also apply for the loss modulus  $G''$ . Nevertheless, the experiments that report stress stiffening of the cytoskeleton versus frequency suffer two main limitations. First, the frequency range of validity of such a law is controversial: it is reported to be  $10^{-2} - 10^3$  Hertz [3], while later articles argue that a different "soft glass" regime occurs at long time scales of physiological interest (above 0.01 s) [4]. Second, the experiments are carried out in a regime of small displacement, where linear analysis applies. A living cell without any external load is able to produce by itself a tensional state that depends on a number of external factors; such an active stress is large enough to place the cellular material in a fully nonlinear regime. Linearized analysis should therefore be carried out with major care because it depends, by definition, on the equilibrium around which small perturbations are applied.

The application of a small force per unit surface to a cell which is not in a relaxed state because of active strain can yield a misintepretation of the results, as shown in Figure 1. From an experimental viewpoint, the mechanical characterization is usually performed applying a force on cells spreading on some specific substrate, typically polyacrilamide. Living cells are well known to produce a stress field when adhering to a surface that strongly depends on its stiffness and adhesivity. This *active* stress can be even quantitatively evaluated by inversion techniques [6], it has a magnitude ranging from tenths to thousands of Pascals so that the external loads actually superpose to it. Thus, two dynamical actors concur to the apparent dynamics and, in principle, it is not clear how to distinguish between them. One possibility is to treat the cell with drugs knocking out specific cytoskeletal components [7, 8]. On the other side, a time scale separation exists: the active cytoskeletal remodeling, at least in fibroblasts, starts after 250 s [9] and one can suitably exploit it to decouple passive and active mechanics in the data.

The dependence of the cellular traction on the specific adhering substrate can be somehow ruled out by optical stretching of suspended cells [10]. A cell is stretched between two laser beams and the deformation is caused by an optically induced surface stress, which can be well modulated changing the incidence angle.

Floating cells are not in a stress free configuration [11], but their tensional state is well reproducible and relatively large force per unit surface can be applied, according to standard

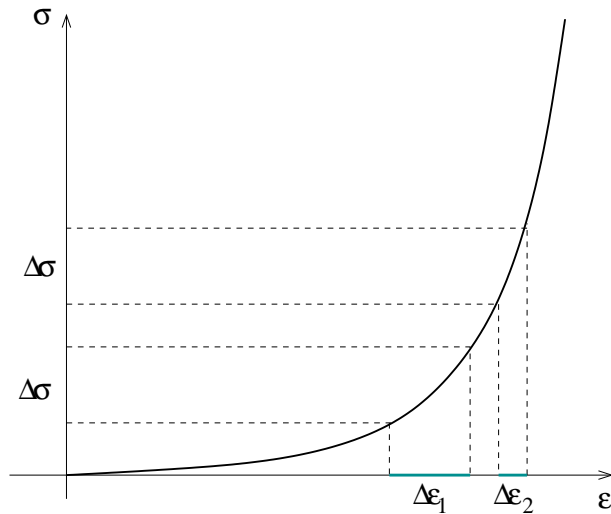


Figure 1: Cells laying on materials of different stiffness actively produce different stresses [5]. Because of the strong nonlinearity in the mechanical response of the cytoskeleton, the same load  $\Delta\sigma$ , externally applied to a cell having different degrees of active pre-stress, produces different incremental strains  $\Delta\epsilon_1$  and  $\Delta\epsilon_2$ .

creep and relaxation protocols. Intriguingly, the experiments by Käs and coworkers [12] reveal plastic rearrangements of the material: after load release the cell does not return to its original configuration and preserves a strained state. Notice that this is true in the time scale of experiments, suitably fixed to be shorter than the time triggering the active reorganization.

The plastic behavior resulting from optical stretching tests has been observed in also other experimental settings and discussed in terms of fiber-reinforcement and fluidization of the cytoskeleton [13]. Intriguingly, the stiffening–softening behavior observed in whole cell mechanics is qualitatively reproduced *in vitro* by a minimalist reconstituted cytoskeletal network (F-actin/HMM): the observed bending of the stress–strain elliptic curves and the dependence on the slope on the cycle (see Figure 1 in [14]) are the basic evidences of a stiffening–softening behavior that can be predicted by the inelastic glassy worm-like chain model.

In this paper we revisit the nowadays classical experiments of optical stretching using a macroscopic theory based on finite visco-elasto-plasticity of soft material, which does not take into account polymeric dynamics neither in a direct nor in a reconstructed way. Inelastic theories are still rather unexplored in cell mechanics, with the remarkable exception of the work by Fernandez and Ott [15]. These authors control the elongation over time of a fibroblast adhering between two microplates, both in terms of a step-in-time stretch and by imposing an elongation growing linearly in time. Their observation time is 5 minutes, which is much longer than the one explored by Wottawah et al. [12]. Exploring stretches up to 100%, they demonstrate that the mechanical behavior of a cell is definitely nonlinear, whilst the linear theory only applies for small perturbations, possibly around a fixed

large deformation. The specific dynamical role of the cytoskeletal connections is elucidated by an experiment of glutaraldehyde fixation of the cross links that prevents slippage: the force-length plot of this rheologically constrained system exhibits the characteristic exponential behavior of fiber-reinforced soft tissues. They also observe that the elastic energy storage depends on the stretching rate, thus suggesting that a suitable inelastic theory should be proposed in order to account for evolving plastic thresholds. In their article, Fernandez and Ott [15] derive an elasto-plastic mathematical model for reproducing their experimental mechanical responses.

Following an analogous modelling approach based on thermodynamical arguments, here we outline a finite visco-elasto-plastic model able to reproduce the optical stretch tests of suspended cells reported by Wottawah and coworkers [12]. The stretch and relaxation of the cell in this frameworks occur within 6-25 seconds. In this time range, the active reorganization of the cytoskeleton has not yet been triggered, so that we can uniquely focus on the passive cellular response.

## 2. Theoretical model and numerical results

In this section we propose a theoretical model for describing the passive behavior of cells observed in optical stretching experiments. First, we review the experimental results and discuss the peculiar characteristics in passive cell mechanics that should be taken into account. Second, we define a finite visco-elasto-plastic model on the basis of thermodynamic arguments, supported by a suitable plastic hardening law. Finally, we compare the theoretical results with the experimental curves, discussing the predictive ability of the proposed model.

### 2.1. Passive cell behavior in optical stretching experiments

A careful insight of the experiments by Wottawah and coworkers [12], corresponding to the circles plotted in Figure 2, reveals the complexity of the passive cell dynamics. Three particular characteristics can be observed and are listed below.

1. When loaded with a sudden stress  $\sigma$  between 15 and 17 Pa, the cell elongates very fast (immediately, in the time scale of the experiments' sampling) to a strain  $\epsilon = (\ell - \ell_0)/\ell_0$  that strongly depends on the applied tension. In particular, increasing the external traction from 15 to 17 Pa, the relative elongation passes from  $\epsilon = 0.4$  to  $\epsilon = 0.65$ . This strong softening of the material is in apparent contrast with exponential strain energies usually adopted for soft living tissues and calls for a different mechanical explanation, at least in the investigated regime.
2. After the initial abrupt strain, the cell starts elongating with the typical exponential saturation curve of a viscoelastic material. The exhibited relaxation time is of the order of 2 seconds.
3. If the load applied on the cell is released, the cell relaxes with a viscoelastic trend analogous to the one observed in the loading phase. During the relaxation step the cell does not recover its initial length, but it asymptotically reaches a different one.

This new length can be dynamically classified as a new "relaxed configuration", as no load is applied. A careful analysis of the experiments reveals that such a relaxed configuration strongly depends both on the applied load value and on the time of the application of the external load.

An attempt to reproduce the observed dynamics by linear spring-dashpot models faces a number of difficulties. The existence of a plateau in the loading stage suggests that the material is basically a solid; roughly speaking, no dashpots in series can be effectively included in the model. Conversely, in the unloading phase the system does not recover the base configuration, so that no standard elastic elements can reproduce the data. The asymptotic plateau cannot be explained in terms of very long relaxation times that, in a linear theory, should intervene in the creep phase too.

The asymptotic value of the deformation is different in the three experiments and it apparently depends both on the applied load and on the total time it has been applied. However, the difference in strain between the peak deformation and the final one is nearly constant in the three cases and it is about  $\Delta\epsilon = 0.035$ . This observation suggests that the power of the external forces provides energy per unit time that can be stored by the material composing the cell only up to a definite amount in form of recoverable energy, the rest being dissipated at microstructural level [16].

## 2.2. Definition of a finite visco-elasto-plastic model

Let us consider a mapping  $\mathbf{x} = \chi(\mathbf{X}, t)$  describing the deformation of the cell from its reference position  $\mathbf{X}$  to its actual configuration in  $\mathbf{x}$  at time  $t$ . The plastic behavior of the material can be modeled using a multiplicative decomposition of the deformation gradient  $\mathbf{F} = \partial\mathbf{x}/\partial\mathbf{X}$  [17], so that:

$$\mathbf{F} = \mathbf{F}_e \mathbf{F}_p \quad (1)$$

where  $\mathbf{F}_p$  represents the plastic deformation of the reference configuration, and  $\mathbf{F}_e$  is the elastic deformation. According to Eq.(1), the partly irreversible scenario in the experiments is modeled representing the cell as a viscoelastic solid, characterized an apparent (visible) deformation  $\lambda = \ell/\ell_0$  that is actually the product of two contributions of different physical nature: the micro-structurally driven (unrecoverable) elongation  $\lambda_p$  times the elastic strain that can be recovered after unloading  $\lambda_e$ , such that:

$$\lambda = \lambda_e \lambda_p \quad (2)$$

The free energy per unit volume  $\bar{\Psi}$  of the cell must depend only on the purely elastic deformation, and the following material functional dependence can be postulated [18]:

$$\bar{\Psi}(\lambda_e) = \Psi(\mathbf{F}_e) - p(\det(\mathbf{F}_e) - 1) \quad (3)$$

where  $p$  is the Lagrange multiplier arising when enforcing the incompressibility of the elastic deformation, which can be calculated from the boundary conditions.

Although the deformation of a spherical cell by side stress is expected to produce, in general,

a non-homogeneous strain, as a first investigation step we assume here uniform deformation and axial symmetry. The plastic deformation is assumed to be volume-preserving, so that the finite plastic deformation gradient in the principal directions read:

$$\mathbf{F}_p = \text{diag}(\lambda_p, 1/\sqrt{\lambda_p}, 1/\sqrt{\lambda_p}); \quad \mathbf{F}_e = \text{diag}(\lambda_e, 1/\sqrt{\lambda_e}, 1/\sqrt{\lambda_e}) \quad (4)$$

Considering the cell in isothermal conditions during the optical stretching, the local form of the second law of thermodynamics by neglecting the thermal contributions reads:

$$\dot{\bar{\Psi}} - \mathbf{T} : \dot{\mathbf{F}} \leq 0 \quad (5)$$

where  $\mathbf{T}$  is the first Piola-Kirchhoff stress tensor inside the cell. Substituting Eqs.(1,3) in Eq.(5), the reduced dissipation inequality rewrites:

$$\left( \mathbf{F}\mathbf{T} - \mathbf{F}_e \frac{\partial \bar{\Psi}}{\partial \mathbf{F}_e} \right) : (\dot{\mathbf{F}}_e \mathbf{F}_e^{-1}) + (\mathbf{F}_p \mathbf{T} \mathbf{F}_e) : (\dot{\mathbf{F}}_p \mathbf{F}_p^{-1}) \geq 0 \quad (6)$$

where  $\mathbf{F}_p \mathbf{T} \mathbf{F}_e$  is the so-called Mandel stress in the intermediate configuration (i.e. the new relaxed configuration after plastic deformation), which is the stress measure driving the evolution of material plasticity [19].

Identifying the principal elastic stretches,  $\lambda_{e1} = \lambda_e$  and  $\lambda_{e2} = \lambda_{e3} = 1/\sqrt{\lambda_e}$ , if the cell is subjected to a uniform uniaxial tension  $T_{11} = T$ , by few calculations the reduced dissipation inequality (6) can be simplified as:

$$\left[ T\lambda - \left( \lambda_{e1} \frac{\partial \bar{\Psi}}{\partial \lambda_{e1}} - \lambda_{e2} \frac{\partial \bar{\Psi}}{\partial \lambda_{e2}} \right) \right] \frac{\dot{\lambda}_e}{\lambda_e} + (T - \lambda_e) \dot{\lambda}_p \geq 0 \quad (7)$$

where it has been used the relation  $T_{22} = T_{33} = 0$  from the stress-free boundary conditions. The cell is here assumed to behave as a neo-Hookean elastic material, so that the strain energy density specifies to:

$$\bar{\Psi} = \frac{\mu}{2} (\lambda_{e1}^2 + \lambda_{e2}^2 + \lambda_{e3}^2 - 3) = \frac{\mu}{2} \left( \lambda_e^2 + \frac{2}{\lambda_e} - 3 \right) \quad (8)$$

where  $\mu$  is the elastic shear modulus. The inequality (7) is always satisfied if both terms are non-negative. At this step we require that both terms in (7) provide a non-negative contribution. The simplest admissible evolution law for the elastic deformation that is admissible from a point of view of such a dissipation principle is

$$\gamma \dot{\lambda}_e = T\lambda - \mu \left( \lambda_e^2 - \frac{1}{\lambda_e} \right) \quad (9)$$

where  $\gamma$  is a viscosity-like coefficient, so that  $\tau_v = \mu/\gamma$  is the characteristic viscoelastic time of the model. Using the same argument, a positive second term at the left hand



side of (7) is ensured if we adopt the following stress-driven dissipative law for the plastic deformation:

$$\dot{\lambda}_p = \frac{1}{\tau_p} (T - T_0)_+ \lambda_e \quad (10)$$

where the symbol  $(\cdot)_+$  denotes the positive part of the argument and  $\tau_p$  dictates the timescale of the plastic rearrangement. Equation (10) states that the rest length  $\lambda_p$  evolves over time depending on the excess stress  $(T - T_0)_+$ , where  $T_0 > 0$  is the threshold of the transition between elastic and plastic regimes. This means that for small traction, the reference elongation of the elastic element does not change. If the stress in the material exceeds this threshold, the rest length grows, in order to preserve the amount of stored elastic energy within the maximum allowed range.

Equation (9) expresses the viscoelastic behavior of the cell: when the load is released, the system returns the (possibly evolved) relaxed state  $\lambda = \lambda_p$ . Equation (10) describes the irreversible dynamics: when the term in between the parentheses is positive (i.e. the system is under sufficiently large tension),  $\lambda_p$  evolves. The difference between the applied load  $T$  and the threshold stress  $T_0$  triggers the plastic reorganization.

The large difference in the apparent asymptotic state reached after loading the cell with similar forces (15 and 17 Pa, respectively) can be reconciled with the nonlinear stress-strain relation that characterizes soft tissues only in a regime of evolving yield stress. Assuming that the threshold stress evolves in time with the plastic strain rate, the usual *hardening* law of the inelastic theory applies:

$$\dot{T}_0 = \delta (\dot{\lambda}_p)^\beta. \quad (11)$$

Some physical insight of the equations is provided by the small-stress case and by the asymptotic value predicted by the model for a sufficiently long time. For moderate loads the relaxed length  $\lambda_p = 1$  at any time and the system behaves as a neo-Hookean material. For large enough loads  $T$ , the cross bonds in the actin network start flowing, the cell creeps and, because of the hardening mechanism, after a sufficiently long time the system reaches the new equilibrium configuration

$$\frac{\mu}{\lambda_p} \left( \lambda_e - \frac{1}{\lambda_e^2} \right) = T = T_0 \quad (12)$$

$$\lambda_p = \frac{1}{\delta} \int_0^\infty (\dot{T}_0)^{1/\beta} dt' \quad (13)$$

According to equation (12), in the final loaded state the tension balances the external force and is equal to the plastic threshold stress. The rest elongation  $\lambda_p$  is provided by (13) in terms of the history of the extra stress.

In the recovery phase ( $T = 0$ ) after a sufficiently long time the system returns the equilibrium configuration  $\lambda_e = 1$ , where the reference strain  $\lambda_p$  has been frozen at the asymptotic value of the loading phase according to equation (13). The irreversibility and

the evolutive nature of equation (11) makes the relaxed configuration  $\lambda_p$  dependent both on the applied load  $T$  and on the loading time and rate, a theoretical prediction in very agreement with the experiments.

The nonlinear mathematical model provided by equations (2),(9), (10) and (11) is more complex than the linear spring-dashpot systems that are usually adopted in the rheological literature, even when dependent on the frequency. We emphasize that nonlinearity is an essential ingredient to account for the apparent irreversibility of the system. The signature of irreversibility resides in the different behaviors exhibited in the loading and unloading phases: when the cell is put in tension, it rapidly extends elastically but even if the load is rapidly released, a residual strain remains. No linear viscoelastic law can account for such an asymmetry between loading and unloading curves.

### *2.3. Numerical simulations and discussion of the results*

Numerical approximation of the solution of the system of first order equations (9), (10) and (11) has been carried out by a fourth order Runge-Kutta algorithm using the following values of the parameters:  $\mu = 120$  Pa,  $\gamma = 130$  Pa s,  $\tau_p = 8$  s,  $\beta = 1.17$  Pa,  $T_0(t = 0) = 14.7$  Pa and  $\delta = 50$  Pa s $^{\beta-1}$ .

The experimental (circles) data are plotted versus the numerical ones (line) in Figure 9. These are standard creep-relaxation tests, with different loads applied for different time intervals (see caption). The error bars in the experimental data (not shown here) report an homogeneous uncertainty equal to  $\pm 0.01$  in strain.

Several features of the observed behavior are well captured by the model. In particular, the final non-zero relaxed configuration and the peak in elongation are correctly predicted. A specific feature exhibited by this mechanical system is the strong difference in strain for two quite near values of stress at very short times (compare plots b and c for  $t \ll 1$  s): the cell elongates up to 0.06 times of length for an applied stress of 17 Pa, while the strain is only 0.04 for the very near load of 15 Pa. This difference is well captured by the model and the inner mechanism of this behavior is in the strongly nonlinear function in  $\lambda_p$  at the right hand side of (11).

Finally, we observe that the fitted mechanical parameter  $\gamma = 130$  Pa s corresponds to the value that can be extrapolated from the reptation time of actin filaments [20], suggesting that the actin cytoskeleton plays a key role in the fluid-to-solid transition of stretched cells.

## **3. Conclusion**

The novel contribution of this work is a different theoretical insight to the complex mechanical behavior of living cells. At the considered time scales, the actomyosin dynamics is supposed to give a negligible contribution and the micromechanical focus is on the role of actin bonds slippage. Without any attempt to upscale the dynamics of the actin fibers at a macro level, setting the ideas of Fernandez and Ott [15] in a precise thermodynamical framework, we straightforwardly apply classical methods of finite visco-elasto-plasticity to account for the experimental behavior of optically stretched cells. Compared to the

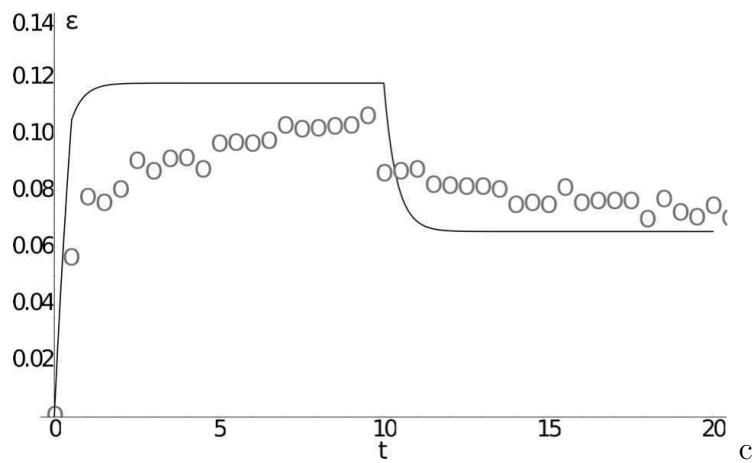
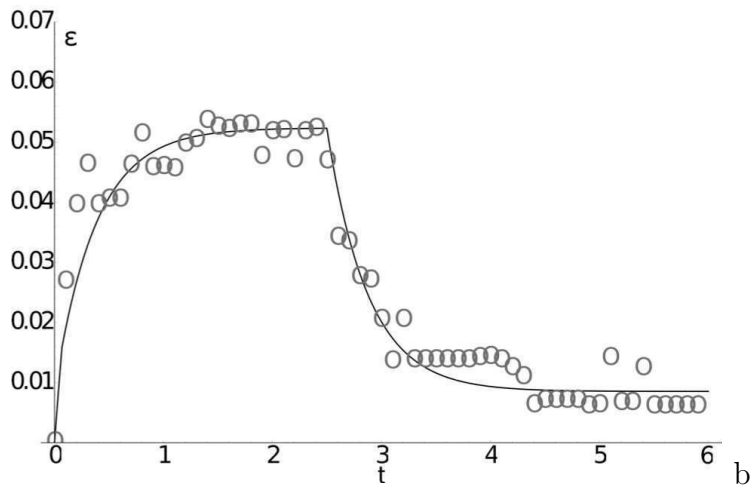
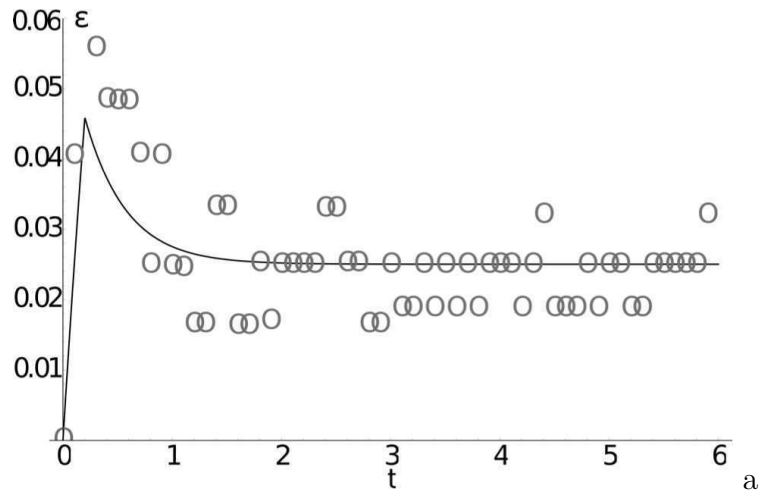


Figure 2: Experimental and theoretically predicted strain plots versus time for a cell. The applied load is 17 Pa for 0.2 s (top), 15 Pa for 2.5 s (middle) and 17 Pa for 15 s (bottom). The error bars in the experimental data are not shown here, but report an homogeneous uncertainty equal to  $\pm 0.01$  in strain.

previously cited work, our model involves less independent fields and parameters to be fitted, ensuring thermodynamical consistency at finite deformations, while its applications to the classical experiments of optical cell stretching reproduces the measures data with a very good agreement.

## Acknowledgments

DA gratefully acknowledges the partial support of the PRIN project *Mathematics and Mechanics of Biological Assemblies and Soft Tissues*.

## References

- [1] Pullarkat PA, Fernandez PA and Ott A, Rheological properties of the Eukaryotic cell cytoskeleton, *Physics Reports* 449:29–53 (2007).
- [2] Hoffman BD and Crocker JC, Cell mechanics: dissecting the physical responses of cells to force, *Annu. Rev. Biomed. Eng.*, 11:259-288 (2009).
- [3] Fabry B, Maskym GN, Butler JP, Glogauer M, Navajas D, Taback NA, Millet EJ and Fredberg JJ, Time scale and other invariants of integrative mechanical behavior in living cells, *Phys. Rev. E* 68 041941 (2003).
- [4] Deng L, Trepast X, Butler JP, Millet E, Morgan KG, Weitz DA and Fredberg JJ, Fast and slow dynamics of the cytoskeleton, *Nature Materials*, 5:636–640 (2006).
- [5] Lo CM, Wang HB, Dembo M and Wang YL, Cell movement is guided by the rigidity of the substrate, *Biophys. J.*, 79:144-152 (2000).
- [6] Dembo M, Oliver T, Ishihara A and Jacobson K, Imaging the traction stresses exerted by locomoting cells with elastic substratum method, *Biophysical J.*, 70:2008-2022 (1996).
- [7] Wakatsuki T, Kolodney MS, Zahalak GI, and Elson EL, Cell mechanics studied by a reconstituted model tissue, *Biophys. J.*, 79:2353–2368 (2000).
- [8] Marquez JP, Elson EL and Genin GM, Whole cell mechanics of contractile fibroblasts: relations between effective cellular and extracellular matrix moduli, *Phil. Trans. R. Soc.*, 368:635–654 (2010)
- [9] Nekouzadeh A, Pryse KM, Elson EL and Genin GM, Stretch-activated force shedding, force recovery, and cytoskeletal remodeling in contractile fibroblasts, *J. Biomechanics* 41:2964–2971 (2008).
- [10] Guck J, Ananthakrishnan R, Mahmood H, Moon TJ, Casey Cunningham J and Käs J, The optical stretcher: a novel laser tool to micromanipulate cells, *Biophys. J.* 81:767-784 (2001).

- [11] Danowski BA, Fibroblast contractility and actin organization are stimulated by microtubule inhibition, *J. Cell Science* 93:255-266 (1989).
- [12] Wottawah F, Schinkinger S, Lincoln B, Ananthakrishnan R, Romeyke M, Guck J and Käs J, Optical Rheology of biological cells, *PRL*, 94:198103 (2005).
- [13] Krishnan R, Park CY, Lin YC, Mead J, Jaspers RT, Trepap X, Lenormand G, Tambe D, Smolensky AV, Knoll AH, Butler JP and Fredberg JJ, Reinforcement versus fluidization in cytoskeletal mechanoresponsiveness, *Plos One* 4(5):e5486 (2009)
- [14] Wolff L, Fernandez P and Kroy K, Resolving the stiffening-softening paradox in cell mechanics, *Plos One* 7(7):e40063 (2012).
- [15] Fernandez P and Ott A, Single cell mechanics: stress stiffening and kinematic hardening, *PRL* 100,2381102 (2008).
- [16] Gurtin ME, Fried E and Lallit A, *The Mechanics and Thermodynamics of Continua*, New York: Cambridge (2010).
- [17] Lee EH, Elastic-plastic deformation at finite strain, *ASME Trans. J. Applied Mech.* 36: 1-6 (1969).
- [18] Epstein M, and Maugin GA., The energy-momentum tensor and material uniformity in finite elasticity, *Acta Mech.* 83: 127-133 (1990).
- [19] Maugin GA, Eshelby stress in elastoplasticity and ductile fracture. *Int. J. Plasticity* 10, 392-408 (1994).
- [20] Spiros A, and Edelstein-Keshet L, Testing a model for the dynamics of actin structures with biological parameter values. *Bull. Math. Biol.* 60, 275-305 (1998).

# MOX Technical Reports, last issues

Dipartimento di Matematica “F. Brioschi”,  
Politecnico di Milano, Via Bonardi 9 - 20133 Milano (Italy)

- 65/2013** AMBROSI, D.; CIARLETTA, P.  
*Plasticity in passive cell mechanics*
- 64/2013** CIARLETTA, P.; AMBROSI, D.; MAUGIN, G.A.  
*Mass transport in morphogenetic processes: a second gradient theory for volumetric growth and material remodeling*
- 63/2013** PIGOLI, D.; MENAFOGLIO, A.; SECCHI, P.  
*Kriging prediction for manifold-valued random field*
- 62/2013** ARIOLI, G.; KOCH, H.  
*Existence and stability of traveling pulse solutions of the FitzHugh-Nagumo equation*
- 61/2013** ANTONIETTI, P.F.; SARTI, M.; VERANI, M.  
*Multigrid algorithms for hp-Discontinuous Galerkin discretizations of elliptic problems*
- 60/2013** GHIGLIETTI, A.; PAGANONI, A.M.  
*An urn model to construct an efficient test procedure for response adaptive designs*
- 59/2013** ALETTI, M.; BORTOLOSSI, A.; PEROTTO, S.; VENEZIANI, A.  
*One-dimensional surrogate models for advection-diffusion problems*
- 58/2013** ARTINA, M.; FORNASIER, M.; MICHELETTI, S.; PEROTTO, S.  
*Anisotropic adaptive meshes for brittle fractures: parameter sensitivity*
- 57/2013** ANTONIETTI, P.F.; PERUGIA, I.; ZALIANI, D.  
*Schwarz domain decomposition preconditioners for plane wave discontinuous Galerkin methods*
- 56/2013** ANTONIETTI, P.F.; AYUSO DE DIOS, B.; MAZZIERI, I.; QUARTERONI, A.  
*Stability analysis for Discontinuous Galerkin approximations of the elastodynamics problem*